iScience

CellPress
OPEN ACCESS

Article

Gold-catalyzed highly enantioselective cycloadditions of 1,6-enynes and 1,6-diynes assisted by remote hydrogen bonding interaction

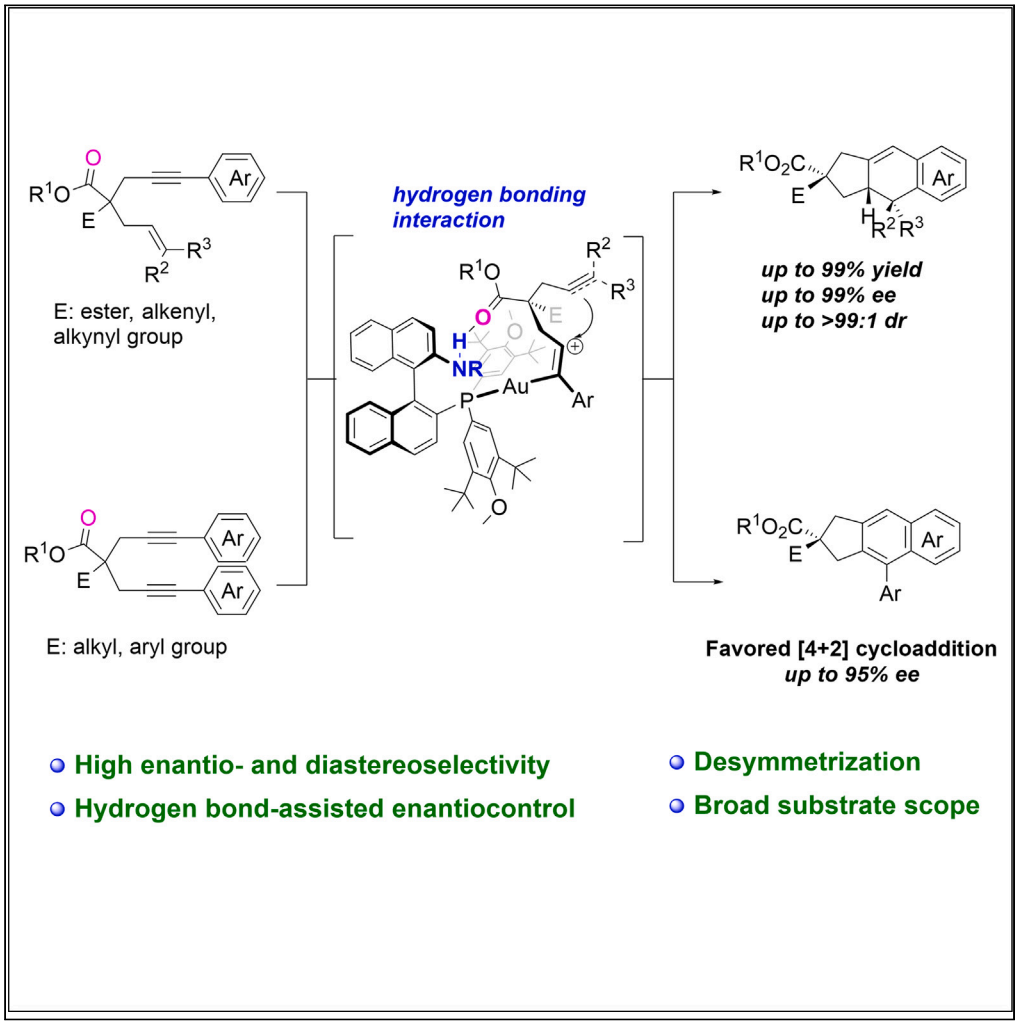

Bijin Lin, Ye Xiao, Tilong Yang, Gen-Qiang Chen, Xumu Zhang, Chi-Ming Che

chengq@sustech.edu.cn (G.-Q.C.)
zhangxm@sustech.edu.cn (X.Z.)
cmche@hku.hk (C.-M.C.)

Highlights

Precise enantioinduction assisted by remote hydrogen bonding interaction

Ester group at the tether of substrates acts as directing group

Desymmetric cycloadditions of 1,6-enynes and 1,6-diynes

Lin et al., iScience 27, 110876 October 18, 2024
https://doi.org/10.1016/j.isci.2024.110876

iScience

CellPress
OPEN ACCESS

Article

Gold-catalyzed highly enantioselective cycloadditions of 1,6-enynes and 1,6-diynes assisted by remote hydrogen bonding interaction

Bijin Lin,[1,2] Ye Xiao,[1] Tilong Yang,[4] Gen-Qiang Chen,[3,*] Xumu Zhang,[2,*] and Chi-Ming Che[1,2,5,*]

SUMMARY

Gold(I)-catalyzed highly enantioselective [4 + 2] cycloadditions of 1,6-enynes were achieved by utilizing chiral bifunctional P,N ligand. A wide range of 1,6-enynes were converted to enantioenriched 5-6-6-fused tricyclic compounds under mild reaction condition (up to 99% ee). This chiral gold(I) complex was also employed in the first desymmetric cycloadditions of 1,6-diynes bearing single ester group at the tether (up to 93% ee), where 5-*exo-dig* pathway predominates over 6-*endo-dig* pathway. DFT calculations and control experiments were performed to rationalize the origin of precise stereocontrol. It implies that hydrogen bonding interaction between the ester group of substrates and the secondary amine of the chiral P,N ligands plays a pivotal role in the control of enantioselectivity. The utilities of the current reaction were demonstrated by scale-up experiment and derivatizations.

INTRODUCTION

In the past two decades, the realm of asymmetric gold(I) catalysis[1–7] has witnessed significant advancements, despite the inherent challenge posed by the linear coordinate geometry of Au(I) catalysts.[8–11] These achievements are predominantly attributed to the employment of chiral ligands[12–15] and chiral counterions[16–18] to impose asymmetric steric hindrance. However, large steric hindrance generally slows reaction and leads to the need for higher catalyst loadings. Attractive noncovalent interaction in asymmetric organocatalysis[19] and asymmetric transition metal catalysis[20,21] has proved successful for many rate accelerations and stereoinduction improvement. Therefore, incorporating a remote noncovalent interaction site onto a chiral ligand scaffold presents a promising strategy for new-generation ligand design in asymmetric gold(I) catalysis.[22] The attractive noncovalent interaction between catalyst and substrate could ensure more precise stereochemical information transfer from the ligand to reactive center. Representative examples in line with this ligand design concept include the chiral ferrocenyl phosphine ligand reported by Ito et al.[23] and chiral bifunctional ligands designed by Zhang et al.[24] (Figure 1A). The noncovalent interaction site could serve as hydrogen-bond acceptor to participate in the enantiodetermining step. In our previous work on gold-catalyzed desymmetric lactonization of alkynylmalonic acids, secondary amine of chiral bifunctional P,N ligand plays a similar role to accept proton (Figure 1B).[25] It was proposed that the secondary amine engages in the ion pairing interaction with the carboxyl group of alkynylmalonic acid to improve stereocontrol. Notedly, hydrogen bond donor is also widely certificated as the key element for stereoinduction improvement in tremendous asymmetric organocatalysis[26–29] and transition metal catalysis.[21,30–35] Actually, the secondary amine could also act as a hydrogen bond donor.

Gold-catalyzed [4 + 2] cycloaddition of 1,6-enyne was first reported by Echavarren et al. in 2005 (Figure 1C).[36,37] The asymmetric version of such reaction provides a straightforward approach to construct chiral 5-6-6-fused tricyclic rings (an important type of structural core in natural products[38–46]), with the first examples being reported by Michelet et al. by employing traditional chiral bisphosphine ligands.[47] Echavarren et al. recently achieved the asymmetric version for various substrates by designing a series of chiral ligands featuring a remote C_2-symmetric diarylpyrrolidine moiety to encapsulate substrate,[48,49] which allows attractive π-π interactions between catalyst and substrate, and also by a modular and tunable strategy that combines achiral gold catalyst featuring hydrogen bond donor and chiral H-bonded counterion.[50] We notice that the tethers of the 1,6-enynes employed in these gold-catalyzed reactions generally bear geminal-diester and or -diether groups to facilitate cyclization due to the Thorpe-Ingold effect.[37] From a new perspective, we envision that these ester groups could also be utilized to distinguish the prochiral carbon center through hydrogen bonding interaction with an NH group of gold(I)-bound chiral P,N ligand in the enantiodetermining step. Here, we report the use of chiral bifunctional P,N ligand in gold(I)-catalyzed asymmetric [4 + 2] cycloaddition of 1,6-enynes bearing geminal-diester groups at the tethers (Figure 1D) with enantioselectivity of up to 99% ee. Also reported here are gold(I)-catalyzed highly enantio- and diastereoselective desymmetric [4 + 2] cycloadditions of 1,6-enynes, each containing two identical

[1]Department of Chemistry, State Key Laboratory of Synthetic Chemistry, The University of Hong Kong, Pokfulam Road, Hong Kong 999077, China
[2]Department of Chemistry, Southern University of Science and Technology, Shenzhen 518055, China
[3]Academy for Advanced Interdisciplinary Studies and Department of Chemistry, Southern University of Science and Technology, Shenzhen 518055, China
[4]Department of Chemistry, The Hong Kong University of Science and Technology, Clear Water Bay, Kowloon, Hong Kong 999077, China
[5]Lead contact
*Correspondence: chengq@sustech.edu.cn (G.-Q.C.), zhangxm@sustech.edu.cn (X.Z.), cmche@hku.hk (C.-M.C.)
https://doi.org/10.1016/j.isci.2024.110876

A Noncovalent interaction sites participating in asymmetric gold catalysis

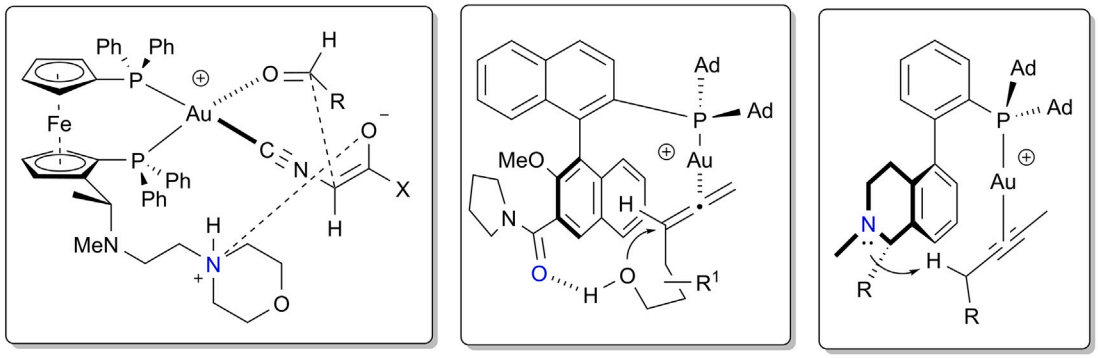

B Gold-catalyzed desymmetric lactonization of alkynylmalonic acids

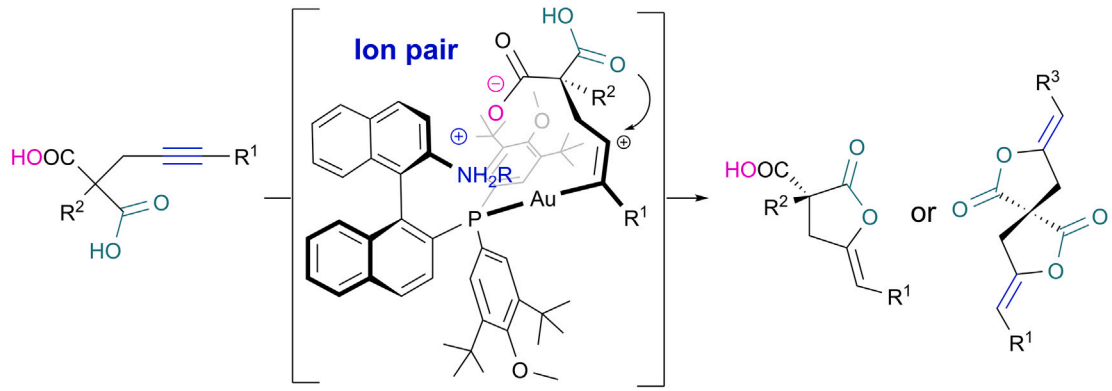

C Gold-catalyzed asymmetric [4+2] cycloaddition of 1,6-enynes

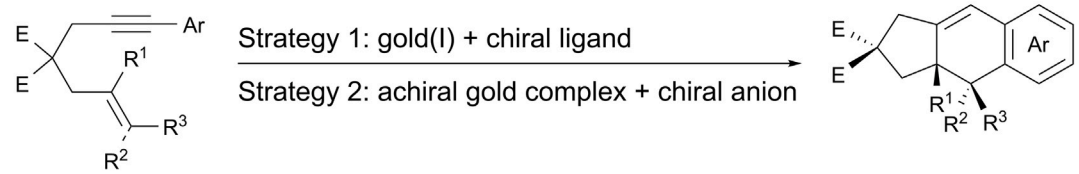

D *This work*: Gold-catalyzed asymmetric cycloadditions of 1,6-enynes and 1,6-diynes

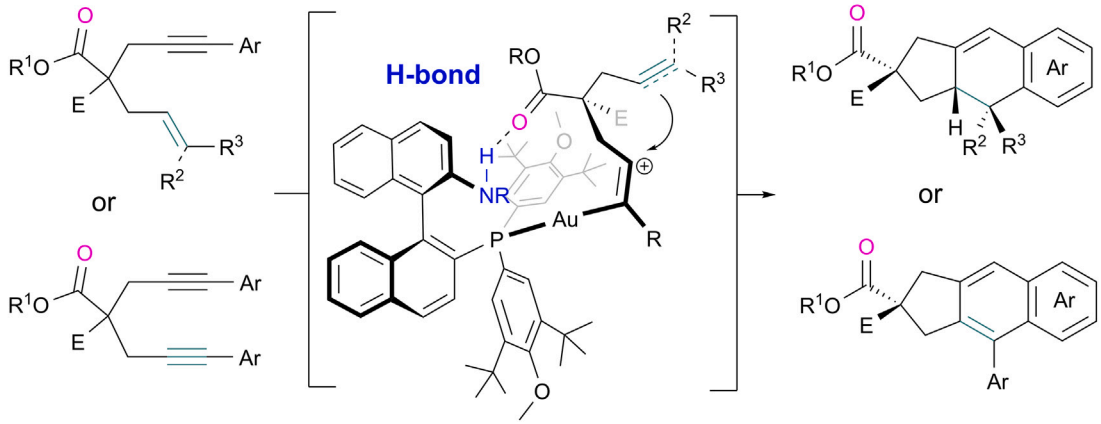

Figure 1. Application of noncovalent interactions in asymmetric gold catalysis
(A) Nonvalent interaction sites participating in asymmetric gold catalysis.
(B) Gold-catalyzed desymmetric lactonization of alkynylmalonic acids.
(C) Gold-catalyzed asymmetric [4 + 2] cycloaddition of 1,6-enynes.
(D) This work: gold-catalyzed asymmetric cycloadditions of 1,6-enynes and 1,6-diynes.

alkenyl or alkynyl groups with a single ester group at the tether (enantioselectivity: up to 99% ee; diastereoselectivity: up to >99:1 dr), together with application in gold-catalyzed cycloaddition of 1,6-diynes[51–56] to provide rare examples of gold(I)-catalyzed asymmetric intramolecular [4 + 2] cycloaddition of 1,6-diynes featuring single ester group at the tether (Figure 1D; enantioselectivity: up to 95% ee).

RESULTS AND DISCUSSION

Reaction condition optimization

In our initial investigation, 1,6-enyne **1a** was chosen as benchmark substrate to optimize reaction conditions (Table S1). The absolute configuration of cycloadduct **2a** was assigned as *R* based on literature characterization of X-ray crystal structure and optical rotation.[50] During the ligand screening (Table S2, see also Schemes S1–S4), *oxa*-spirocyclic P,N ligands[57] **L1**–**L3** (Scheme S1) were initially evaluated; 73% yield and 55% ee were achieved with **L1** bearing primary amine (Table 1, entry 1). By using **L2** and **L3** with secondary amine group instead, the ee values were increased to 70% and 86%, respectively (Table 1, entries 2–3). It indicates that secondary amine of P,N ligands with larger steric hindrance contributes to better enantiomeric induction. While a less sterically hindered binaphthyl P,N ligand[25] **L4** was found to achieve a similarly high enantioselectivity of 87% ee with **L3** (Table 1, entry 4). By changing the aromatic group on the phosphine atom to bulkier DTB substituents (**L5**), enantioselectivity was improved to 96% ee (Table 1, entry 5). To our delight, **L6** featuring more sterically demanding DTBM substituents on phosphine atom achieved 99% ee (Table 1, entry 6; enantioselectivities of 76–93% ee were previously reported for the same reaction using other gold catalysts[47–50,58]). To investigate the important role of secondary amine for enantiocontrol, **L7** (Scheme S2) with primary amine was tested. It still led to high yield, albeit with lower enantioselectivity of 91% ee (Table 1, entry 7). **L8** (Scheme S3) with tertiary amine was also synthesized through methylation of the NH group of **L4**. With **L8**AuCl as the catalyst, the reaction proceeded with poor yield (39%) and enantioselectivity (50% ee) (Table 1, entry 8). Commercially available MOP ligand **L9** was also investigated to give a poor enantioselectivity of 27% ee (Table 1, entry 9). These experiments demonstrate that chiral binaphthyl P,N ligand with larger steric hindered secondary amine contributes to precise enantiocontrol in the asymmetric cycloaddition of 1,6-enynes and the hydrogen bonding interaction that secondary amine of ligand engaged may make a significant influence on the enantiocontrol. Subsequently, we evaluated the effect of various solvents (Table S1) and chloride scavengers (Table S3) with **L6**AuCl as catalyst for the model reaction (Table 1, entries 10–17). Nonpolar solvent toluene and $AgSbF_6$ stand out as the optimal solvent and chloride scavenger. In contrast to the high enantioselectivity achieved by using toluene as the solvent, poor enantioselectivity was observed upon using polar solvent THF (Table 1, entry 12). The obvious solvent effect further illustrates the importance of hydrogen bonding interaction in the enantiocontrol. To evaluate the stability of **L6**AuCl, the catalyst loading was reduced to 0.5 mol% and 0.2 mol% (Table S4). Full conversion (99% yield) was achieved with 98% ee and 95% ee, respectively (Table 1, entries 18–19). Therefore, **L6**AuCl proved to be a highly selective and robust gold catalyst for the model reaction.

Scope for asymmetric gold(I)-catalyzed cycloaddition of 1,6-enynes

Under the optimal reaction conditions, the substrate scope of the **L6**AuCl-catalyzed cycloaddition of 1,6-enynes (**1**, Scheme S5) was examined (Scheme 1). Substrates 1,6-enynes **1a**–**1c** with geminal-di(methyl ester), -di(ethyl ester), and –diether groups, respectively, all underwent a formal [4 + 2] cycloaddition smoothly, affording fused tricyclic compounds **2a**–**2c** in 94%–99% yields. Substrates **1a** and **1b** with geminal-diester groups at the tether afforded **2a** and **2b** with 99% ee and 98% ee, respectively, significantly higher than the 49% ee obtained for **2c** bearing geminal-diether groups at the tether, probably because ether group acts as less effective hydrogen bond acceptor to interact with the secondary amine in **L6**. The cyclization of **1d** and **1e** yielded **2d** with 97% ee (>99:1 dr) and **2e** with 92% ee (96:4 dr), respectively, within 7 h. In literature, by using other gold catalysts, an enantioselectivity of 16% ee was reported for **2e**[58] and enantioselectivities of 86%–91% ee and 62%–78% ee were obtained for the geminal-diether counterparts of **2d** and **2e**, respectively.[49,50] For substrates **1f**–**1h**, each bearing an electron-donating group at the *para* position of the aromatic ring, the reactions gave **2f**–**2h** with 95%–98% ee, higher than those of products **2i**–**2k** (69%–87% ee) obtained from substrates **1i**–**1k** bearing electron-withdrawing *para*-substituents. Fused tricyclic compounds possessing *meta*- and *ortho*-substituents (**2l**–**2n**) were also synthesized (from substrates **1l**–**1n**) with high yields (92%–98%) and enantioselectivity (94%–97% ee). Gratifyingly, 1,6-enynes featuring 1-naphthyl, 3-benzothiophenyl, 3-thiophenyl, and 2-thiophenyl substituents at the alkynyl terminus were also tolerated in the reaction to afford cycloadducts **2o**–**2r** in 91%–98% yields and 97%–99% ee.

The utilization of chiral bifunctional P,N ligand in the gold(I)-catalyzed formal [4 + 2] cycloaddition of 1,6-enynes **1** achieved high enantioselectivity through discriminating the enantiotopic faces of alkene. To examine the directing effect of the tethered ester group in the stereoinduction, we prepared 1,6-enynes **3** featuring a prochiral quaternary carbon center with a single ester group and two identical alkenyl (Scheme S6) or alkynyl groups (Scheme S7).[59] Under the standard reaction conditions, 1,6-enynes **3a**–**3c**, each bearing two allyl groups, and **3d** bearing two propargyl moieties underwent desymmetric [4 + 2] cycloaddition smoothly to give 5-6-6-fused tricyclic compounds **4a**–**4d** with excellent enantioselectivity and diastereoselectivity (97%–99% ee, up to >99:1 dr) (Scheme 2). Notedly, the reaction of **3c** shows high regioselectivity in the process of Friedel-Crafts-type cyclization to give a single cycloadduct **4c**. The relative configuration of **4a** and **4d** was determined by H-H COSY, NOESY, HSQC, and HMBC analysis. The putative hydrogen bonding interaction between ester group of

Table 1. Selected condition screening for enantioselective [4 + 2] cycloadditions of 1,6-enyne 1a to give 2a

Entry[a]	Ligand	Solvent	Additive	Yield (%)[b]	Ee (%)[c]
1	L1	Toluene	$AgSbF_6$	73	55
2	L2	Toluene	$AgSbF_6$	99	70
3	L3	Toluene	$AgSbF_6$	99	86
4	L4	Toluene	$AgSbF_6$	74	87
5	L5	Toluene	$AgSbF_6$	99	−96
6	L6	Toluene	$AgSbF_6$	99	99
7	L7	Toluene	$AgSbF_6$	99	91
8	L8	Toluene	$AgSbF_6$	39	50
9	L9	Toluene	$AgSbF_6$	81	27
10	L6	CH_2Cl_2	$AgSbF_6$	97	89
11	L6	DCE	$AgSbF_6$	98	88
12	L6	THF	$AgSbF_6$	90	31
13	L6	Toluene	$AgPF_6$	40	75
14	L6	Toluene	$AgBF_4$	29	79
15	L6	Toluene	$AgNTf_2$	5	–
16	L6	Toluene	AgOTf	68	73
17	L6	Toluene	NaBArF	60	40
18[d]	L6	Toluene	$AgSbF_6$	99	98
19[e]	L6	Toluene	$AgSbF_6$	99	95

[a]Reaction conditions: **1a** (0.1 mmol), LAuCl/$AgSbF_6$ (1 mol %), toluene (0.1 M), room temperature, 4–48 h.
[b]Yields of **2a** were determined by ^{1}H NMR using dibromomethane as internal standard.
[c]Enantiomeric excesses (ee) were determined by HPLC analysis using a chiral stationary phase.
[d]0.5 mol % of catalyst loading was used.
[e]0.2 mol % of catalyst loading was used.

substrates and secondary amine group of chiral P,N ligand could account for the precise enantiocontrol in the discrimination of the enantiotopic carbon center at the tether and influence the subsequent stereodetermining electrophilic addition toward the enantiotopic face of alkene, resulting in high diastereoselectivity. This desymmetric variation of [4 + 2] cycloaddition reaction provides a direct approach to access 5-6-6-fused tricyclic compounds featuring a quaternary stereocenter. In order to demonstrate the practical utility of our catalytic system, the effect of the catalytic loading of **L6**AuCl for the reaction of **3a** was evaluated (see Table S4 in the supplemental information for details). Increasing the S/C to 500 could maintain a high level of enantioselectivity (98% ee). When the S/C was further increased to 2,000, full conversion was achieved within 2 days, albeit with slightly lower enantioselectivity of 91% ee.

Due to the simultaneous existence of the prochiral face and center in 1,6-enynes **3**, the mutual influence cannot be ruled out. Thus, 1,6-diynes **5** (Scheme S8) with single ester group at the tether were also examined with this gold catalytic system (Scheme 3). During the reaction condition optimization with **5a** (see Table S5 in the supplemental information for more details), it was shown that no reaction took place using chiral bisphosphine ligands. However, utilizing chiral P,N ligands **L5** and **L6** with secondary amine could achieve full conversion, albeit with competition between [4 + 2] and [3 + 2] cycloadditions, resulting in mixed products of **6a** and **6a′** in the ratio of 4.4:1 and 4.6:1, respectively. When chiral P,N ligand **L7** with tertiary amine was employed instead, no reaction occurred either. It was demonstrated that the NH group of chiral P,N ligands could facilitate this transformation. Ultimately, **L5** and **L6** turn out to be privileged ligands in terms of reactivity and enantioselectivity. In contrast to the [3 + 2] cycloaddition of 1,6-diynes reported by Liu et al.,[60] the desymmetric cycloadditions of 1,6-diynes **5a**–**5c** with our catalytic system tend to afford [4 + 2]-cycloadduct as major product. Overall, [4 + 2]-cycloadducts **6a**–**6c** were obtained with higher enantioselectivities (91%–95% ee) than [3 + 2]-cycloadducts **6a′**–**6c′** (48%–80% ee). The reaction for 1,6-diyne **5c** with a bulkier phenyl group on prochiral carbon center afforded [4 + 2]-cycloadducts with higher enantioselectivity than the reaction for **5a** and **5b**. The regioselectivities (**6**:**6′**) vary from 1.8:1 to 5.3:1. The absolute configuration of **6c** was determined to be (*S*) by X-ray diffraction analysis (Tables S6 and S7). In comparison with the reaction of 1,6-enynes, the cycloadditions of 1,6-diynes require longer time. Therefore, 1,6-diynes exhibit relatively lower reactivity under current reaction condition.

To demonstrate the application potential, we carried out the scale-up experiment of **3a** under standard reaction condition, and **4a** was obtained in high yield with retention of high enantio- and diastereoselectivity (302 mg, 93% yield, 98% ee, >99: dr) (Scheme 4). The chiral 5-6-6-fused tricyclic compound **4a** can be hydrolyzed under basic condition to carboxylic acid **7a** without loss of high enantioselectivity and diastereoselectivity (97% ee, >99:1 dr). Furthermore, **4a** with two different alkene moieties can also be selectively derivatized to bromohydrin **8a** (91% yield, 1:1.5 dr) in the presence of NBS and DMSO/H_2O or to epoxide **9a** with *m*-CPBA as oxidant (55% yield, 1:1 dr).

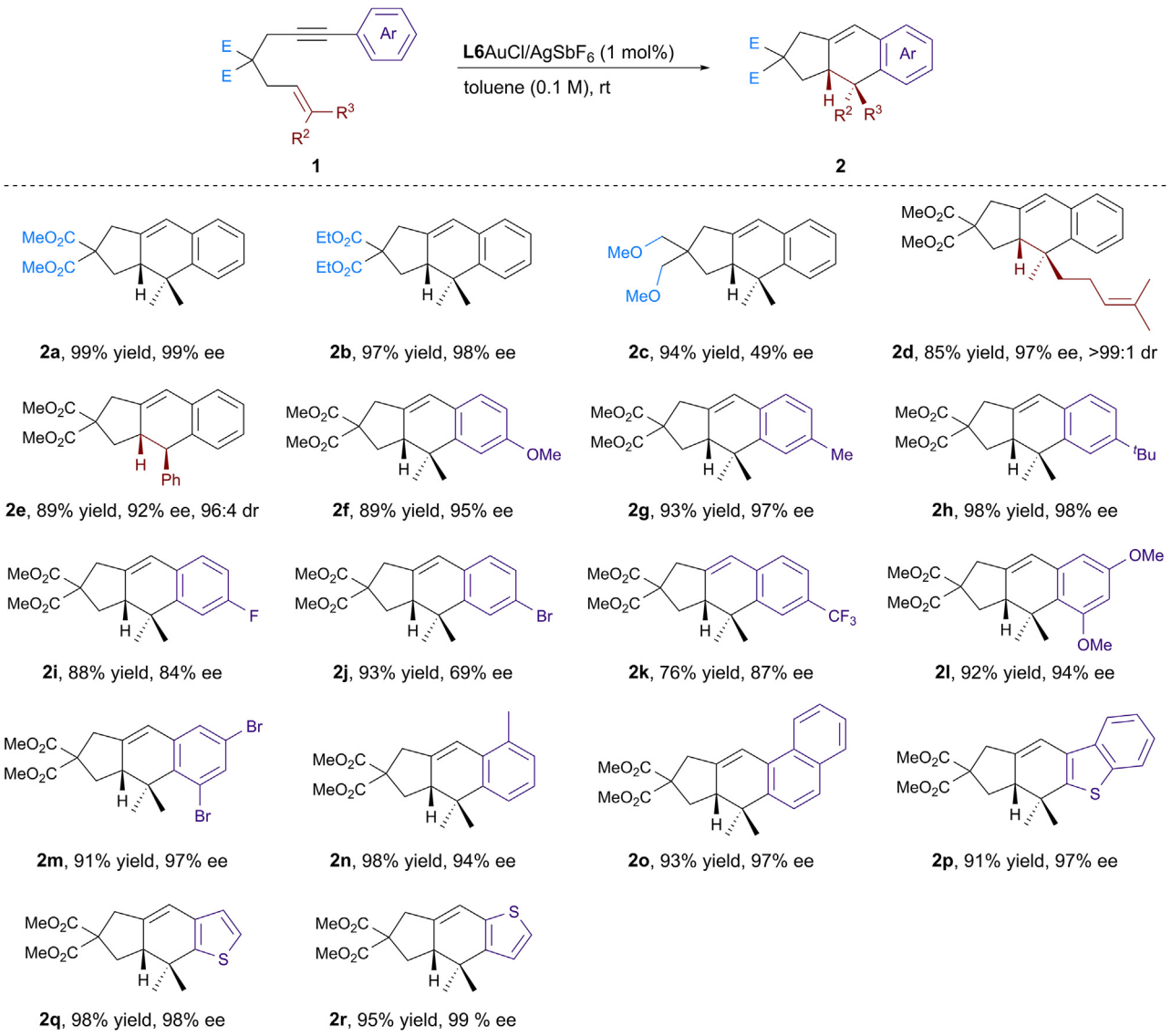

Scheme 1. Asymmetric gold(I)-catalyzed cycloaddition of 1,6-enynes

Reaction conditions: **1** (0.1 mmol), **L6**AuCl/$AgSbF_6$ (1 mol %), toluene (0.1 M), room temperature, 2–24 h. All reactions were monitored by TLC. Isolated yields were reported. Enantiomeric excesses (ee) of **2** were determined by HPLC using a chiral stationary phase.

To better rationalize the origin of enantioselectivity, DFT calculations were conducted on the model [4 + 2] cycloaddition of **1a** with **L6**AuCl (Figure 2). Based on previously reported DFT calculations, it was assumed that nucleophilic attack of either the *Re* or the *Si* enantiotopic face of the alkene toward the Au(I)-activated alkyne was the enantiodetermining step, leading to the formation of cyclopropyl Au(I) carbene intermediates.[49,50] Comparing the two transition states TS_R and TS_S (Data S1), (η^2-alkyne)gold(I) complex preferentially undergoes *anti*-attack by the *Re*-prochiral face of the alkene. As shown in TS_R, the distance between NH of **L6**AuCl and C=O of **1a** is 2.06 Å, which is in the range of hydrogen bond.[61] However, the expected hydrogen bond is not shown between NH and C=O in **TSs** but occurred between NH and OMe with a distance of 2.08 Å. The Gibbs energy difference between two transition states ($\Delta\Delta G^{\ddagger}_{R\text{-}S}$) is 3.3 kcal/mol, i.e., 99% ee. The result supports the explanation that the hydrogen bonding interaction between ligand and substrate accounts for excellent discrimination of the enantiotopic alkene face in the enantiodetermining step. In other words, gold and secondary amine act as two hands to clamp the substrate molecule. Since the enantiotopic center bearing ester motif has been desymmetrized by secondary amine moiety in chiral catalyst cave, the neighboring enantiotopic face of alkene is also affected, leading to high diastereoselectivity. Therefore, the chirality transfer is more efficient with the bifunctional P,N ligand, decreasing the steric demand for rather crowded environment. Applying the calculated enantiocontrol model outlined in TS_R and substituting **1a** with **5c**, where the free ester group was replaced by a phenyl

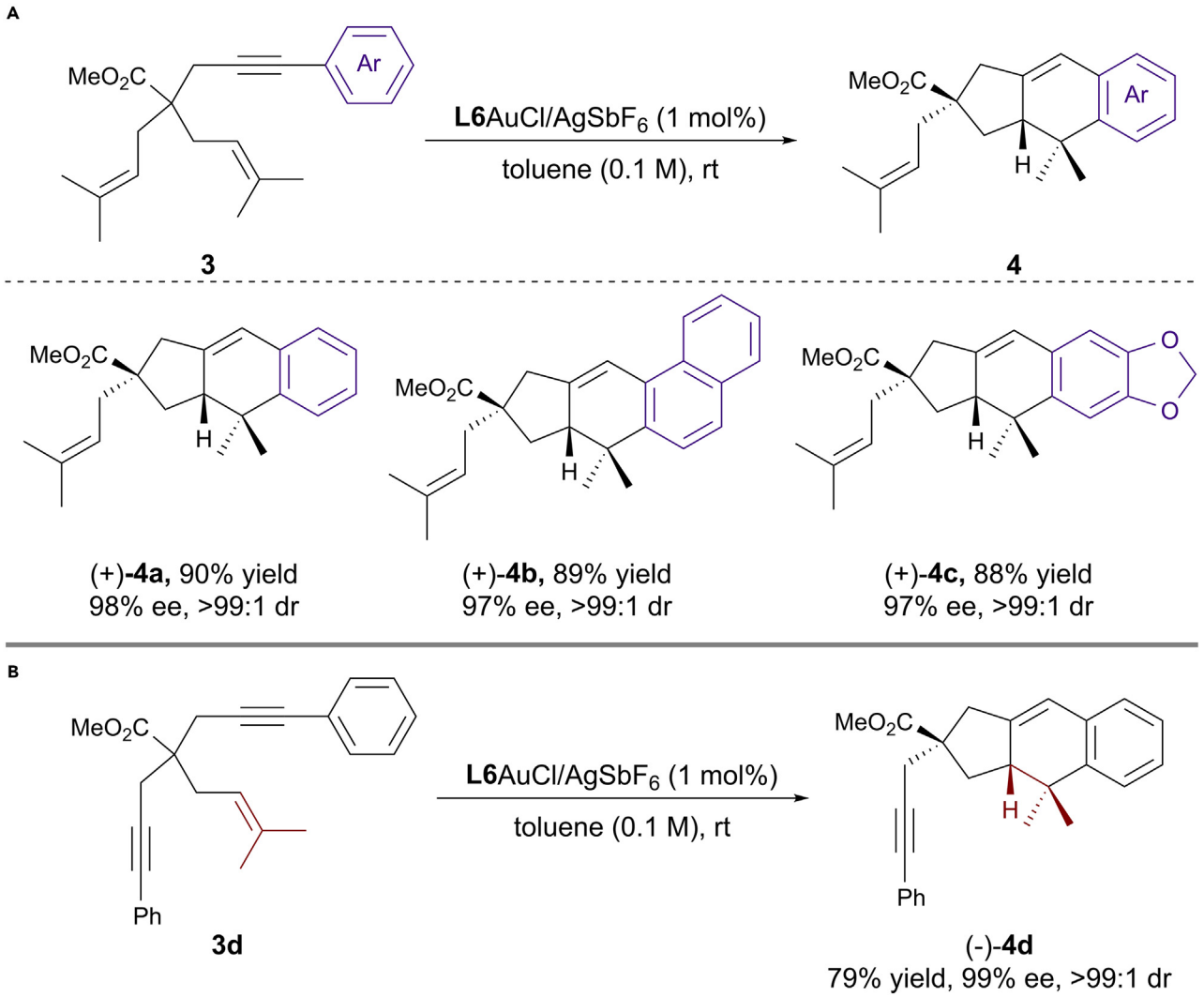

Scheme 2. Gold(I)-catalyzed desymmetric cycloaddition of 1,6-enynes

Reaction conditions: **3** (0.1 mmol or 0.2 mmol), **L6**AuCl/$AgSbF_6$ (1 mol %), toluene (0.1 M), room temperature, 6–12 h. Enantiomeric excesses (ee) of **4** were determined by HPLC using a chiral stationary phase. Isolated yields were reported.

(A) Reaction of 1,6-enynes bearing two identical alkenyl groups.

(B) Reaction of 1,6-enyne bearing two identical alkynyl groups.

group and the alkenyl group was replaced by an identical alkynyl group, lead to the formation of (*S*)-**6c**. The predicted configuration of **6c** is consistent with the experimental result.

In conclusion, gold-catalyzed asymmetric [4 + 2] cycloadditions of 1,6-enynes by employing a chiral binaphthyl-based P,N ligand resulted in excellent enantioselectivity and diastereoselectivity under mild reaction conditions, providing various 5-6-6-fused tricyclic compounds with up to 99% ee and up to 99:1 dr. Furthermore, gold-catalyzed first desymmetric [4 + 2] cycloaddition of 1,6-diynes featuring single ester group at the tether was also achieved firstly with high enantioselectivity and moderate regioselectivity. The putative H-bonding interaction between NH moiety of P,N ligand and carbonyl group of substrates could account for the precise enantiocontrol. Control experiments and DFT calculations elucidate the essential role of secondary amine group in the ligand and the probable engagement of hydrogen bonding interaction in the enantiodetermining step. The outstanding performance of the attractive noncovalent interaction assistance in enantiocontrol deserves to be further explored in the future of asymmetric gold catalysis.

Limitations of the study

Although the desymmetric cycloaddition of 1,6-diynes exhibited excellent enantioselectivity, it still needs to further improve the regioselectivity by developing a more powerful asymmetric catalytic system.

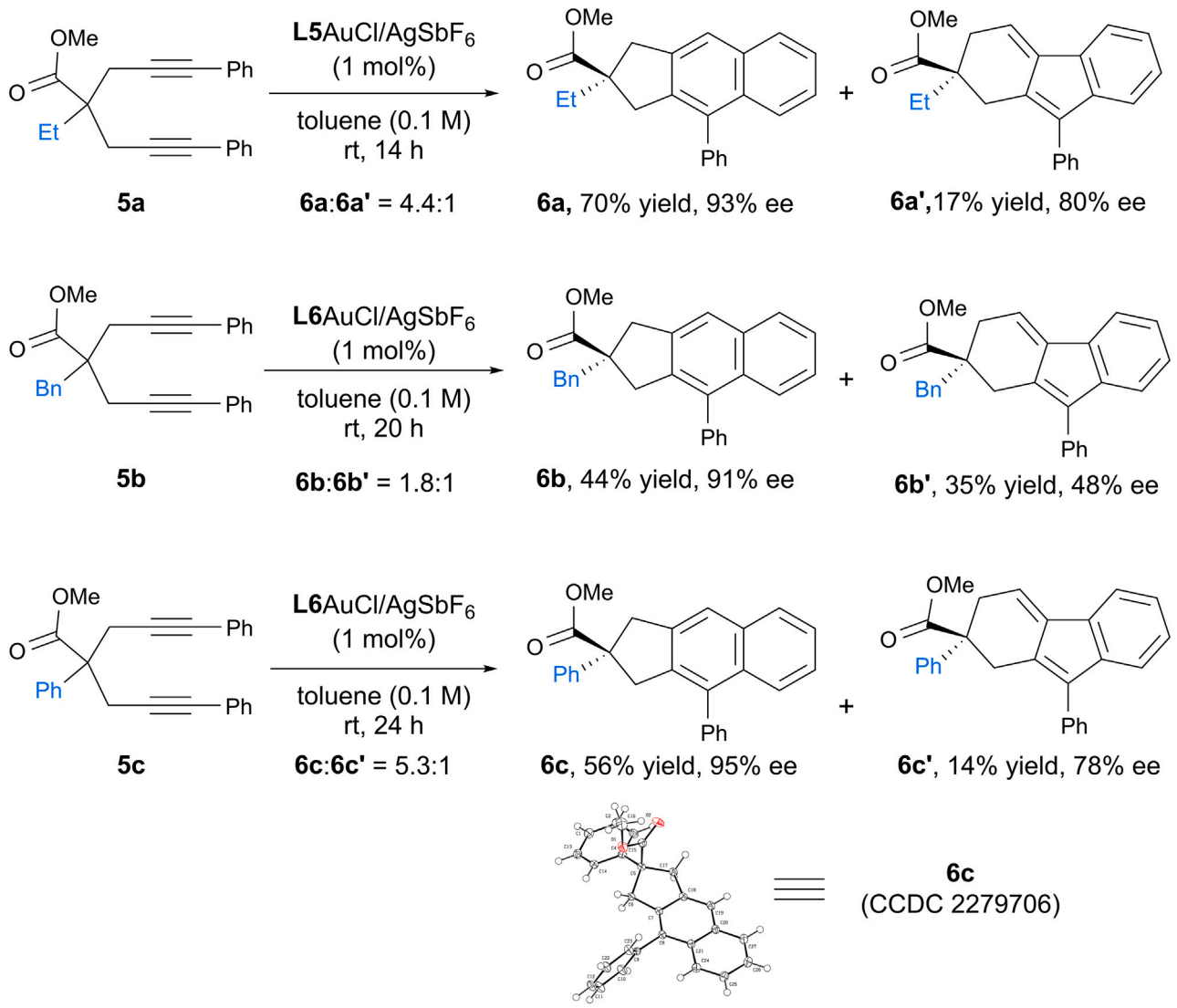

Scheme 3. Gold(I)-catalyzed desymmetric cycloaddition of 1,6-diynes

Reaction conditions: **5** (0.1 mmol or 0.2 mmol), **L5**AuCl/$AgSbF_6$ or **L6**AuCl/$AgSbF_6$ (1 mol %), toluene (0.1 M), room temperature. Isolated yields were reported. Enantiomeric excesses (ee) of **6** were determined by HPLC using a chiral stationary phase. See also Table S5 for the crystal data of compound (*S*)-**6c**.

RESOURCE AVAILABILITY

Lead contact

Further information and requests for resources should be directed to and will be fulfilled by the lead contact, Chi-Ming Che (cmche@hku.hk).

Materials availability

All materials generated in this study are provided in the supplemental information. Where available, these may be shared by the lead contact.

Data and code availability

- All data reported in this paper have been deposited and publicly available as of the date of publication. Accession numbers are listed in the key resources table.
- This paper does not report original code.
- Any additional information required to reanalyze the data reported in this paper can be obtained from the lead contact upon request.

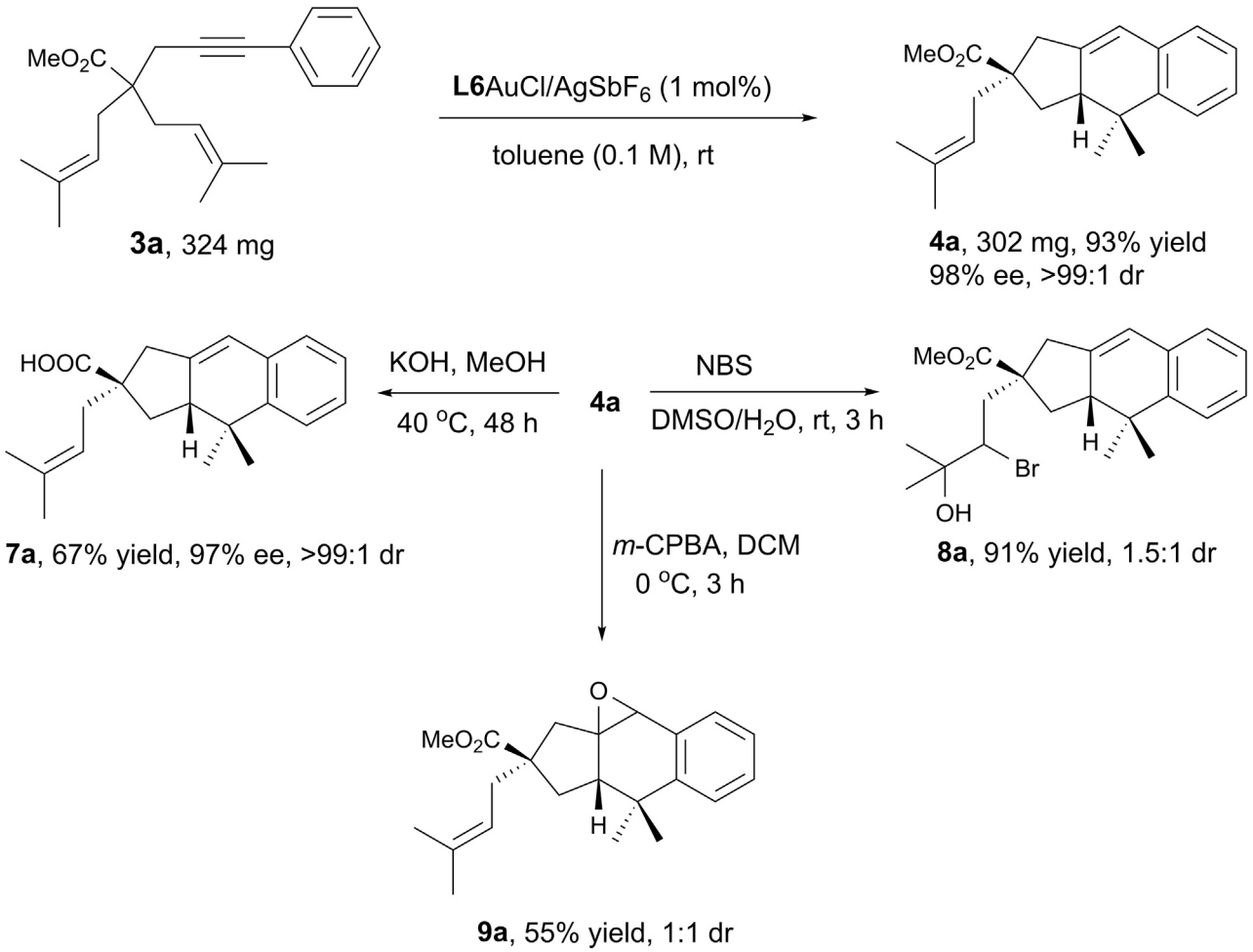

Scheme 4. Scale-up experiment and derivatizations.

ACKNOWLEDGMENTS

This work was supported by the grants from the Innovation and Technology Commission (HKSAR, China) to the State Key Laboratory of Synthetic Chemistry and from the Laboratory for Synthetic Chemistry and Chemical Biology under the Health@InnoHK Program launched by the Innovation and Technology Commission, the Government of HKSAR. We thank Dr. Xiaoyong Chang (Southern University of Science and Technology) for assistance in X-ray crystallographic analysis. Computational work was supported by Center for Computational Science and Engineering at Southern University of Science and Technology (SUSTech). The authors acknowledge the assistance of SUSTech Core Research Facilities.

AUTHOR CONTRIBUTIONS

C.-M.C. and X.Z. conceived and supervised the study; B.L. designed the experiments and analyzed the data; B.L. and Y.X. conducted the experiments; G.-Q.C. performed the DFT calculations; T.Y. provided suggestion on DFT calculations; B.L. and G.-Q.C. wrote the manuscript.

DECLARATION OF INTERESTS

The authors declare no competing interests.

STAR★METHODS

Detailed methods are provided in the online version of this paper and include the following:

- KEY RESOURCES TABLE
- METHOD DETAILS
  - General procedure for enantioselective [4 + 2] cycloaddition of 1,6-enynes
  - General procedure for desymmetric cycloaddition of 1,6-diynes
  - Theoretical methodology

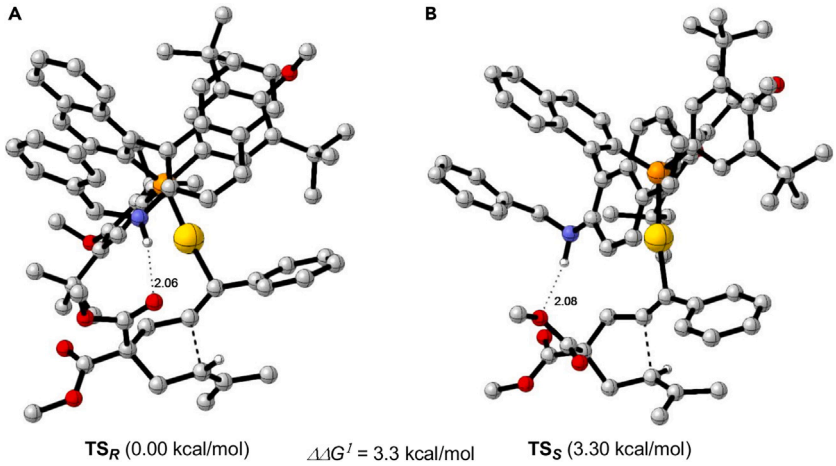

Figure 2. DFT-calculated transition state (TS) geometries for gold-catalyzed [4 + 2] cycloaddition of 1a using L6AuCl

(A) Transition state TS_R.

(B) Transition state TS_S.

SUPPLEMENTAL INFORMATION

Supplemental information can be found online at https://doi.org/10.1016/j.isci.2024.110876.

Received: February 28, 2024
Revised: June 14, 2024
Accepted: August 30, 2024
Published: September 2, 2024

REFERENCES

1. Huguet, N., and Echavarren, A.M. (2012). Asymmetric Gold-Catalyzed Reactions (Wiley-VCH Verlag GmbH & Co. KGaA).
2. Toullec, P.Y., Pradal, A., and Michelet, V. (2014). Recent Developments in Asymmetric Catalysis (Georg Thieme Verlag).
3. Brill, M., and Nolan, S.P. (2018). Chiral Carbophilic Gold Lewis Acid Complexes in Enantioselective Catalysis (Springer GmbH).
4. Widenhoefer, R.A. (2008). Recent developments in enantioselective gold(I) catalysis. Chem. Eur J. *14*, 5382–5391. https://doi.org/10.1002/chem.200800219.
5. Zi, W., and Toste, F.D. (2016). Recent advances in enantioselective gold catalysis. Chem. Soc. Rev. *45*, 4567–4589. https://doi.org/10.1039/C5CS00929D.
6. Li, Y., Li, W., and Zhang, J. (2017). Gold-catalyzed enantioselective annulations. Chem. Eur J. *23*, 467–512. https://doi.org/10.1002/chem.201602822.
7. Jiang, J.-J., and Wong, M.-K. (2021). Recent advances in the development of chiral gold complexes for catalytic asymmetric catalysis. Chem. Asian J. *16*, 364–377. https://doi.org/10.1002/asia.202001375.
8. Hashmi, S.K., and Toste, F.D. (2012). Modern Gold Catalyzed Synthesis (Wiley-VCH Verlag GmbH & Co. KGaA).
9. Slaughter, L.M. (2015). Homogeneous Gold Catalysis (Springer).
10. Hashmi, A.S.K. (2021). Introduction: Gold Chemistry. Chem. Rev. *121*, 8309–8310.
11. Herrera, R.P., and Gimeno, M.C. (2021). Main Avenues in Gold Coordination Chemistry. Chem. Rev. *121*, 8311–8363. https://doi.org/10.1021/acs.chemrev.0c00930.
12. Michelet, V., Pradal, A., and Toullec, P. (2011). Recent Developments in Asymmetric Catalysis in the Presence of Chiral Gold Complexes. Synthesis *2011*, 1501–1514. https://doi.org/10.1055/s-0030-1258465.
13. Cera, G., and Bandini, M. (2013). Enantioselective Gold(I) Catalysis with Chiral Monodentate Ligands. Isr. J. Chem. *53*, 848–855. https://doi.org/10.1002/ijch.201300029.
14. Wang, Y.-M., Lackner, A.D., and Toste, F.D. (2014). Development of Catalysts and Ligands for Enantioselective Gold Catalysis. Acc. Chem. Res. *47*, 889–901. https://doi.org/10.1021/ar400188g.
15. Mishra, S., Urvashi, and Patil, N.T. (2022). Chiral Ligands for Au(I), Au(III), and Au(I)/Au(III) Redox Catalysis. Isr. J. Chem. *63*, e202200039. https://doi.org/10.1002/ijch.202200039.
16. Inamdar, S.M., Konala, A., and Patil, N.T. (2014). When gold meets chiral Bronsted acid catalysts: extending the boundaries of enantioselective gold catalysis. Chem. Commun. *50*, 15124–15135. https://doi.org/10.1039/C4CC04633A.
17. Jia, M., and Bandini, M. (2015). Counterion Effects in Homogeneous Gold Catalysis. ACS Catal. *5*, 1638–1652. https://doi.org/10.1021/cs501902v.
18. Bao, M., Zhou, S., Hu, W., and Xu, X. (2022). Recent advances in gold-complex and chiral organocatalyst cooperative catalysis for asymmetric alkyne functionalization. Chin. Chem. Lett. *33*, 4969–4979. https://doi.org/10.1016/j.cclet.2022.04.050.
19. Knowles, R.R., and Jacobsen, E.N. (2010). Attractive Noncovalent Interactions in Asymmetric Catalysis: Links Between Enzymes and Small Molecule Catalysts. Proc. Natl. Acad. Sci. USA *107*, 20678–20685. https://doi.org/10.1073/pnas.1006402107.
20. Fanourakis, A., Docherty, P.J., Chuentragool, P., and Phipps, R.J. (2020). Recent Developments in Enantioselective Transition Metal Catalysis Featuring Attractive Noncovalent Interactions between Ligand and Substrate. ACS Catal. *10*, 10672–10714. https://doi.org/10.1021/acscatal.0c02957.
21. Zhao, Q., Chen, C., Wen, J., Dong, X.-Q., and Zhang, X. (2020). Noncovalent Interaction-Assisted Ferrocenyl Phosphine Ligands in Asymmetric Catalysis. Acc. Chem. Res. *53*, 1905–1921. https://doi.org/10.1021/acs.accounts.0c00347.
22. Zuccarello, G., Escofet, I., Caniparoli, U., and Echavarren, A.M. (2021). New-Generation Ligand Design for the Gold-Catalyzed Asymmetric Activation of Alkynes. ChemPlusChem *86*, 1283–1296. https://doi.org/10.1002/cplu.202100232.
23. Ito, Y., Sawamura, M., and Hayashi, T. (1986). Catalytic asymmetric aldol reaction: reaction of aldehydes with isocyanoacetate catalyzed by a chiral ferrocenylphosphine-gold(I) complex. J. Am. Chem. Soc. *108*, 6405–6406. https://doi.org/10.1021/ja00280a056.
24. Wang, Z., Nicolini, C., Hervieu, C., Wong, Y.F., Zanoni, G., and Zhang, L. (2017). Remote Cooperative Group Strategy Enables Ligands

for Accelerative Asymmetric Gold Catalysis. J. Am. Chem. Soc. *139*, 16064–16067. https://doi.org/10.1021/jacs.7b09136.
25. Lin, B., Yang, T., Zhang, D., Zhou, Y., Wu, L., Qiu, J., Chen, G.-Q., Che, C.-M., and Zhang, X. (2022). Gold-Catalyzed Desymmetric Lactonization of Alkynylmalonic Acids Enabled by Chiral Bifunctional P,N ligands. Angew. Chem., Int. Ed. *61*, e202201739. https://doi.org/10.1002/anie.202201739.
26. Fuerst, D.E., and Jacobsen, E.N. (2005). Thiourea-Catalyzed Enantioselective Cyanosilylation of Ketones. J. Am. Chem. Soc. *127*, 8964–8965. https://doi.org/10.1021/ja052511x.
27. Banik, S.M., Levina, A., Hyde, A.M., and Jacobsen, E.N. (2017). Lewis acid enhancement by hydrogen-bond donors for asymmetric catalysis. Science *358*, 761–764. https://doi.org/10.1126/science.aao5894.
28. Doyle, A.G., and Jacobsen, E.N. (2007). Small-Molecule H-Bond Donors in Asymmetric Catalysis. Chem. Rev. *107*, 5713–5743. https://doi.org/10.1021/cr068373r.
29. Yu, X., and Wang, W. (2008). Hydrogen-bond-mediated asymmetric catalysis. Chem. Asian J. *3*, 516–532. https://doi.org/10.1002/asia.200700415.
30. Zhao, Q., Li, S., Huang, K., Wang, R., and Zhang, X. (2013). A Novel Chiral Bisphosphine-Thiourea Ligand for Asymmetric Hydrogenation of β,β-Disubstituted Nitroalkenes. Org. Lett. *15*, 4014–4017. https://doi.org/10.1021/ol401816y.
31. Wen, J., Jiang, J., and Zhang, X. (2016). Rhodium-Catalyzed Asymmetric Hydrogenation of α,β-Unsaturated Carbonyl Compounds via Thiourea Hydrogen Bonding. Org. Lett. *18*, 4451–4453. https://doi.org/10.1021/acs.orglett.6b01812.
32. Liu, G., Zhang, H., Huang, Y., Han, Z., Liu, G., Liu, Y., Dong, X.-Q., and Zhang, X. (2019). Efficient synthesis of chiral 2,3-dihydro-benzo[b]thiophene 1,1-dioxides via Rh-catalyzed hydrogenation. Chem. Sci. *10*, 2507–2512. https://doi.org/10.1039/c8sc05397a.
33. Wang, H., Wen, J., and Zhang, X. (2021). Chiral Tridentate Ligands in Transition Metal-Catalyzed Asymmetric Hydrogenation. Chem. Rev. *121*, 7530–7567. https://doi.org/10.1021/acs.chemrev.1c00075.
34. Reek, J.N.H., de Bruin, B., Pullen, S., Mooibroek, T.J., Kluwer, A.M., and Caumes, X. (2022). Transition Metal Catalysis Controlled by Hydrogen Bonding in the Second Coordination Sphere. Chem. Rev. *122*, 12308–12369. https://doi.org/10.1021/acs.chemrev.1c00862.
35. Wang, H.-H., Shao, H., Huang, G., Fan, J., To, W.P., Dang, L., Liu, Y., and Che, C.-M. (2023). Chiral Iron Porphyrins Catalyze Enantioselective Intramolecular C (sp3)−H Bond Amination Upon Visible-Light Irradiation. Angew. Chem., Int. Ed. *62*, e202218577. https://doi.org/10.1002/anie.202218577.
36. Nieto-Oberhuber, C., López, S., and Echavarren, A.M. (2005). Intramolecular [4+2] cycloadditions of 1,3-enynes or arylalkynes with alkenes with highly reactive cationic phosphine Au(I) complexes. J. Am. Chem. Soc. *127*, 6178–6179. https://doi.org/10.1021/ja042257t.
37. Nieto-Oberhuber, C., Pérez-Galan, P., Herrero-Gómez, E., Lauterbach, T., Rodríguez, C., López, S., Bour, C., Rosellón, A., Cardenas, D.J., and Echavarren, A.M. (2008). Gold(I)-Catalyzed Intramolecular [4+2] Cycloadditions of Arylalkynes or 1,3-Enynes with Alkenes: Scope and Mechanism. J. Am. Chem. Soc. *130*, 269–279. https://doi.org/10.1021/ja075794x.
38. Dang, P.H., Nguyen, H.X., Nguyen, H.H.T., Vo, T.D., Le, T.H., Phan, T.H.N., Nguyen, M.T.T., and Nguyen, N.T. (2017). Lignans from the Roots of Taxus wallichiana and Their α-Glucosidase Inhibitory Activities. J. Nat. Prod. *80*, 1876–1882. https://doi.org/10.1021/acs.jnatprod.7b00171.
39. Teponno, R.B., Kusari, S., and Spiteller, M. (2016). Recent advances in research on lignans and neolignans. Nat. Prod. Rep. *33*, 1044–1092. https://doi.org/10.1039/c6np00021e.
40. Lau, W., and Sattely, E.S. (2015). Six enzymes from mayapple that complete the biosynthetic pathway to the etoposide aglycone. Science *349*, 1224–1228. https://doi.org/10.1126/science.aac7202.
41. Laird, D.W., Poole, R., Wikström, M., and Altena, I.A.v. (2007). Pycnanthuquinone C, an unusual 6,6,5-tricyclic geranyltoluquinone from the Western Australian brown alga Cystophora harveyi. J. Nat. Prod. *70*, 671–674. https://doi.org/10.1021/np060566m.
42. Gordaliza, M., García, P.A., del Corral, J.M.M., Castro, M.A., and Gómez-Zurita, M.A. (2004). Podophyllotoxin: distribution, sources, applications and new cytotoxic derivatives. Toxicon *44*, 441–459. https://doi.org/10.1016/j.toxicon.2004.05.008.
43. Wang, B.-G., Ebel, R., Nugroho, B.W., Prijono, D., Frank, W., Steube, K.G., Hao, X.-J., and Proksch, P. (2001). Aglacins A-D, first representatives of a new class of aryltetralin cyclic ether lignans from Aglaia cordata. J. Nat. Prod. *64*, 1521–1526. https://doi.org/10.1021/np0102962.
44. Fort, D.M., Ubillas, R.P., Mendez, C.D., Jolad, S.D., Inman, W.D., Carney, J.R., Chen, J.L., Ianiro, T.T., Hasbun, C., Bruening, R.C., et al. (2000). Novel antihyperglycemic terpenoid-quinones from Pycnanthus angolensis. J. Org. Chem. *65*, 6534–6539. https://doi.org/10.1021/jo000568q.
45. Cambie, R., Pang, G., Parnell, J., Rodrigo, R., and Weston, R. (1979). Chemistry of the Podocarpaceae. LIV. Lignans from the Wood of Dacrydium intermedium. Aust. J. Chem. *32*, 2741–2751. https://doi.org/10.1071/CH9792741.
46. Noguchi, K., and Kawanami, M. (1940). The active components of the Umbelliferae. X. Components of Anthricus sylvestris. Yakugaku Zasshi *60*, 629.
47. Chao, C.-M., Vitale, M.R., Toullec, P.Y., Genêt, J.P., and Michelet, V. (2009). Asymmetric gold-catalyzed hydroarylation/cyclization reactions. Chem. Eur J. *15*, 1319–1323. https://doi.org/10.1002/chem.200802341.
48. Zuccarello, G., Mayans, J.G., Escofet, I., Scharnagel, D., Kirillova, M.S., Perez-Jimeno, A.H., Calleja, P., Boothe, J.R., and Echavarren, A.M. (2019). Enantioselective Folding of Enynes by Gold(I) Catalysts with a Remote C_2-Chiral Element. J. Am. Chem. Soc. *141*, 11858–11863. https://doi.org/10.1021/jacs.9b06326.
49. Caniparoli, U., Escofet, I., and Echavarren, A.M. (2022). Planar Chiral 1,3-Disubstituted Ferrocenyl Phosphine Gold(I) Catalysts. ACS Catal *12*, 3317–3322. https://doi.org/10.1021/acscatal.1c05827.
50. Franchino, A., Martí, À., and Echavarren, A.M. (2022). H-Bonded Counterion-Directed Enantioselective Au(I) Catalysis. J. Am. Chem. Soc. *144*, 3497–3509. https://doi.org/10.1021/jacs.1c11978.
51. Lin, Y., Zhou, T., Guo, W., Teng, Z., and Xia, Y. (2019). The mechanism of the gold-catalyzed intramolecular [3 + 2]-cycloaddition of 1,6-diynes: a DFT study. Dalton Trans. *48*, 5698–5704. https://doi.org/10.1039/c9dt00553f.
52. Li, T., Wang, H., Qian, P., Yang, Y., Li, B., and Zhang, L. (2018). Au(I)-Catalyzed expeditious access to naphtho[2,3-c]furan-1(3-H)-ones from readily available propargylic ynoates. Chem. Commun. *54*, 10447–10450. https://doi.org/10.1039/C8CC06056H.
53. Li, D., Rao, W., Tay, G.L., Ayers, B.J., and Chan, P.W.H. (2014). Gold-Catalyzed Cycloisomerization of 1,6-Diyne Esters to 1H-Cyclopenta[b]naphthalenes, cis-Cyclopenten-2-yl δ-Diketones, and Bicyclo[3.2.0]hepta-1,5-dienes. J. Org. Chem. *79*, 11301–11315. https://doi.org/10.1021/jo5020195.
54. Rao, W., Koh, M.J., Li, D., Hirao, H., and Chan, P.W.H. (2013). Gold-Catalyzed Cycloisomerization of 1,6-Diyne Carbonates and Esters to 2,4a-Dihydro-1H-fluorenes. J. Am. Chem. Soc. *135*, 7926–7932. https://doi.org/10.1021/ja4032727.
55. Candito, D.A., and Lautens, M. (2011). Stereoselective nickel-catalyzed [2 + 2 + 2] cycloaddition of enynes and arynes. Synlett *22*, 1987–1992. https://doi.org/10.1055/s-0030-1261171.
56. Shibata, T., Fujiwara, R., and Takano, D. (2005). Thermal and Au(I)-catalyzed intramolecular [4+2] cycloaddition of aryl-substituted 1,6-diynes for the synthesis of biaryl compounds. Synlett *2005*, 2062–2066. https://doi.org/10.1055/s-2005-871959.
57. Chen, G.-Q., Lin, B.J., Huang, J.M., Zhao, L.Y., Chen, Q.S., Jia, S.P., Yin, Q., and Zhang, X. (2018). Design and synthesis of chiral oxa-spirocyclic ligands for Ir-catalyzed direct asymmetric reduction of Bringmann's lactones with molecular H_2. J. Am. Chem. Soc. *140*, 8064–8068. https://doi.org/10.1021/jacs.8b03642.
58. Pradal, A., Chao, C.-M., Vitale, M.R., Toullec, P.Y., and Michelet, V. (2011). Asymmetric Au-catalyzed domino cyclization/nucleophile addition reactions of enynes in the presence of water, methanol and electron-rich aromatic derivatives. Tetrahedron *67*, 4371–4377. https://doi.org/10.1016/j.tet.2011.03.071.
59. Sturla, S.J., Kablaoui, N.M., and Buchwald, S.L. (1999). A Titanocene-Catalyzed Intramolecular Ene Reaction: Cycloisomerization of Enynes and Dienynes. J. Am. Chem. Soc. *121*, 1976–1977. https://doi.org/10.1021/ja9839567.
60. Lian, J.-J., Chen, P.-C., Lin, Y.-P., Ting, H.-C., and Liu, R.-S. (2006). Gold-Catalyzed Intramolecular [3 + 2]-Cycloaddition of Arenyne-Yne Functionalities. J. Am. Chem. Soc. *128*, 11372–11373. https://doi.org/10.1021/ja0643826.
61. Steiner, T. (2002). Reviews: The hydrogen bond in the solid state. Angew. Chem., Int. Ed. *41*, 48–76. https://doi.org/10.1002/1521-3773(20020104)41:1<48::aid-anie48>3.0.co;2-u.
62. Frisch, M.J., Trucks, G.W., Schlegel, H.B., Scuseria, G.E., Robb, M.A., Cheeseman, J.R., Scalmani, G., Barone, V., Mennucci, B., Petersson, G.A., et al. (2013). Gaussian 09 Revision D.01 (Gaussian Inc.).
63. Ciancaleoni, G., Rampino, S., Zuccaccia, D., Tarantelli, F., Belanzoni, P., and Belpassi, L. (2014). An ab Initio Benchmark and DFT

Validation Study on Gold(I)-Catalyzed Hydroamination of Alkynes. J. Chem. Theor. Comput. *10*, 1021–1034. https://doi.org/10.1021/ct400980w.

64. Kang, R., Chen, H., Shaik, S., and Yao, J. (2011). Assessment of Theoretical Methods for Complexes of Gold(I) and Gold(III) with Unsaturated Aliphatic Hydrocarbon: Which Density Functional Should We Choose? J. Chem. Theor. Comput. *7*, 4002–4011. https://doi.org/10.1021/ct200656p.

65. Garcia-Morales, C., Ranieri, B., Escofet, I., Lopez-Suarez, L., Obradors, C., Konovalov, A.I., and Echavarren, A.M. (2017). Enantioselective Synthesis of Cyclobutenes by Intermolecular [2+2] Cycloaddition with Non-C_2 Symmetric Digold Catalysts. J. Am. Chem. Soc. *139*, 13628–13631. https://doi.org/10.1021/jacs.7b07651.

66. Andrae, D., Huermann, U., Dolg, M., Stoll, H., and Preu, H. (1991). Energy-adjustedab initio pseudopotentials for the second and third row transition elements: Molecular test for M2 (M=Ag, Au) and MH (M=Ru, Os). Theor. Chim. Acta *78*, 247–266. https://doi.org/10.1007/bf01112848.

67. Petersson, A., Bennett, A., Tensfeldt, T.G., Al-Laham, M.A., Shirley, W.A., and Mantzaris, J. (1988). A complete basis set model chemistry. I. The total energies of closed-shell atoms and hydrides of the first-row elements. J. Chem. Phys. *89*, 2193–2218. https://doi.org/10.1063/1.455064.

68. Petersson, G.A., and Al-Laham, M.A. (1991). A complete basis set model chemistry. II. Open-shell systems and the total energies of the first-row atoms. J. Chem. Phys. *94*, 6081–6090. https://doi.org/10.1063/1.460447.

69. Ehlers, A.W., Böhme, M., Dapprich, S., Gobbi, A., Höllwarth, A., Jonas, V., Köhler, K.F., Stegmann, R., Veldkamp, A., and Frenking, G. (1993). A set of f-polarization functions for pseudo-potential basis sets of the transition metals Sc Cu, Y Ag and La Au. Chem. Phys. Lett. *208*, 111–114. https://doi.org/10.1016/0009-2614(93)80086-5.

70. Tomasi, J., Mennucci, B., and Cammi, R. (2005). Quantum Mechanical Continuum Solvation Models. Chem. Rev. *105*, 2999–3093. https://doi.org/10.1021/cr9904009.

STAR★METHODS

KEY RESOURCES TABLE

REAGENT or RESOURCE	SOURCE	IDENTIFIER
Chemicals, Peptides, and Recombinant Proteins		
(*R*)-(+)-2-Diphenylphosphino-2′-methoxy-1,1′-binaphthyl	Leyan	CAS: 145964-33-6
Silver hexafluoroantimonate(V)	Energy Chemical	CAS: 26042-64-8
3-Bromopropyne	Energy Chemical	CAS: 106-96-7
3,3-Dimethylallyl bromide	Energy Chemical	CAS: 870-63-3
Deposited data		
Crystallographic data for the structures of **6c**	Cambridge Crystallographic Data Center (https://www.ccdc.cam.ac.uk).	CCDC 2279706

METHOD DETAILS

General procedure for enantioselective [4 + 2] cycloaddition of 1,6-enynes

1,6-Enyne **1** or **3** (0.1 mmol or 0.2 mmol), **L**AuCl (1 mol %), $AgSbF_6$ (1 mol %) and toluene (0.1 M) were added sequentially to a 4 mL brown reaction vial under argon. The reaction mixture was stirred at room temperature. Upon completion of the reaction, one drop of dimethyl sulfide was added to quench the reaction. Then the resulting solution was concentrated under reduced pressure and purified by preparative TLC (hexane/EA 20:1 v/v) to afford product **2** or **4**.

General procedure for desymmetric cycloaddition of 1,6-diynes

1,6-Diynes **5** (0.2 mmol), **L**AuCl (1 mol %), $AgSbF_6$ (1 mol %) and toluene (0.1 M) were added sequentially to a 4 mL brown reaction vial under argon. The reaction mixture was stirred at room temperature. Upon completion of the reaction, one drop of dimethyl sulfide was added to quench the reaction. Then the resulting solution was concentrated under reduced pressure and the crude residue was purified by preparative TLC (hexane/EA 20:1 v/v) to afford product **6**.

Theoretical methodology

Calculations were performed by means of the Gaussian 16 suite of programs.[62] DFT was applied using BP86-D3 that has proved its efficiency in other DFT studies of gold-catalyzed transformations.[49,63–65] The SDD basis set and ECP was used to describe Au.[66] The 6-31G(d) basis set was employed for all remaining atoms (C, H, P, F, O and N).[67,68] Frequency calculations were carried out for optimized structures to verify the stationary points or transition states at the same level. Polarization functions (ζf = 1.050) were added for Au.[69] Solvent effect of toluene was considered using the PCM mode.[70] Single-point energies were refined with the basis set 6–311++G** using the same functional. Geometric structures of all species were optimized at T = 298.15 K and 1 atm.